J. Am. Ceram. Soc., 68 [3] 120–127 (1985)

Residual Stresses and Cracking in Metal/Ceramic Systems for Microelectronics Packaging

C. H. HSUEH and A. G. EVANS*

Department of Materials Science and Mineral Engineering, University of California, Berkeley, California 94720

Residual stresses that develop in a metal/ceramic system due to thermal expansion mismatch were calculated for a work-hardening metal. The calculations were conducted for a cylindrical configuration, pertinent to certain microelectronics packaging systems. Experimental measurements of the stress have also been made on a Cu/cordierite ceramic system, using an indentation technique. It is shown that porosity in the metal can plastically expand and provide a mode of dilatational relaxation. Porosity in the metal thus emerges as an important stress-relaxing mechanism.

I. Introduction

A NUMBER of applications in microelectronics involve combinations of metal and ceramic constituents. These constituents are typically subject to residual stress due to thermal expansion mismatch. The residual stresses may result in cracks, that impede the electrical performance of the device. The intent of this article is to evaluate the residual stresses that develop (for a sample configuration) and to examine the implications for cracking.

The metal constituent is generally amenable to plastic deformation and hence, the stress analysis is inherently an elastic/plastic problem. The residual stress is thus expected to exhibit dependence on the yield strength and work-hardening coefficient, as well as the mismatch in thermal expansion. However, the specific influence of these material variables on the residual stress depends on the configuration of the system. For present purposes, a cylindrical geometry (Fig. 1) is considered, as pertinent to the conduction element in a microelectronics package.[1]

Residual stresses are calculated for the cylindrical configuration, subject to the premise that processing is conducted at elevated temperatures, where the stresses are fully relaxed. Stresses thus develop upon cooling due to thermal expansion mismatch. Specific stress amplitudes are computed using the material properties for the technologically significant system: copper/cordierite ceramic. The calculations include considerations of temperature-dependent plastic properties and of the influence of porosity, especially in the metal conducting element, on the residual stress.

The residual stress computations are compared with experimental measurements obtained for the copper/cordierite ceramic system. The localized residual stresses are determined by indentation techniques, with indentations placed in the ceramic, adjacent to the metal/ceramic interface (Fig. 2). The plastic properties of the metal required for stress determination are also assessed by indentation methods.

Finally, the implications of the stress analysis for various modes of mechanical failure in the device are discussed. In particular, cracking of the ceramic, debonding of the interface, and ductile fracture/fatigue of the metal are explored by using specific failure criteria pertinent to each situation.

Received April 19, 1984; revised copy received October 25, 1984; approved October 30, 1984.

*Member, the American Ceramic Society.

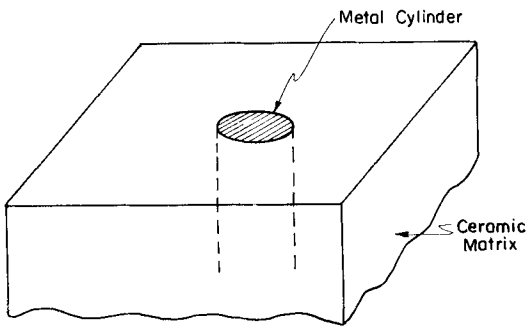

Fig. 1. Geometry used for residual stress analysis: a metal cylinder in an infinite ceramic matrix.

II. Residual Stress Analysis

(1) General Approach

The residual stresses are determined by the usual procedure of first allowing the two constituents to exhibit an unconstrained differential shrinkage, as depicted in Fig. 3 (for a metal with a larger thermal expansion than the ceramic). Then, equal but opposite radial, σ, and axial, σ_z, tractions are placed around the metal and ceramic surfaces (Fig. 3(*C*)) in order to restore displacement continuity at the interface. The tractions are subject to the requirement that the resultant average axial stress be zero since there is no external force on the system and furthermore, in the specific case of an infinite ceramic matrix, the matrix-axial stress, $\sigma_z^c \to 0$.

The attainment of displacement continuity induces elastic strains in the ceramic matrix and both elastic and plastic strains in the metal cylinder. The induced strains in the metal cylinder consist of a dilatation and a distortion. The dilatation contributes stresses that depend primarily on the thermal mismatch strain, while the distortion induces stresses dictated largely by plastic flow stress. These two components are evident in the final solutions for the residual stresses.

The radial and tangential stresses in the infinite ceramic matrix, subject to interface tractions, σ, are given by[2]

$$\sigma_r^c = \sigma(a/r)^2 \tag{1a}$$

$$\sigma_\theta^c = -\sigma(a/r)^2 \tag{1b}$$

where a is the cylinder radius and r is the distance from the axis

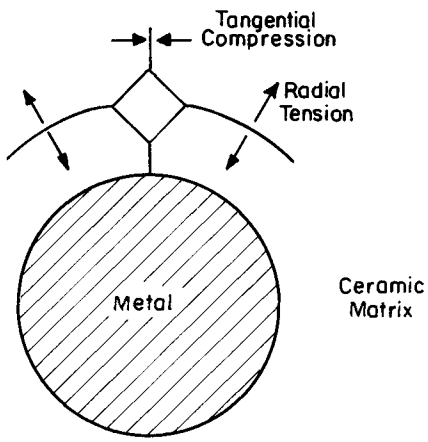

Fig. 2. Schematic illustrating effect of residual stress on indentation cracks.

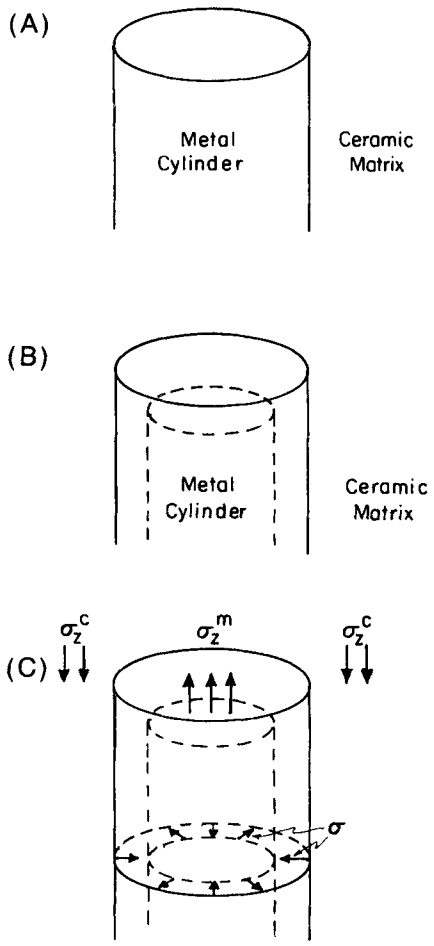

Fig. 3. (*A*) Metal and ceramic bonded at high temperature; (*B*) unconstrained differential shrinkage at room temperature; (*C*) residual stresses that develop to allow displacement and stress continuity due to expansion mismatch between metal and ceramic.

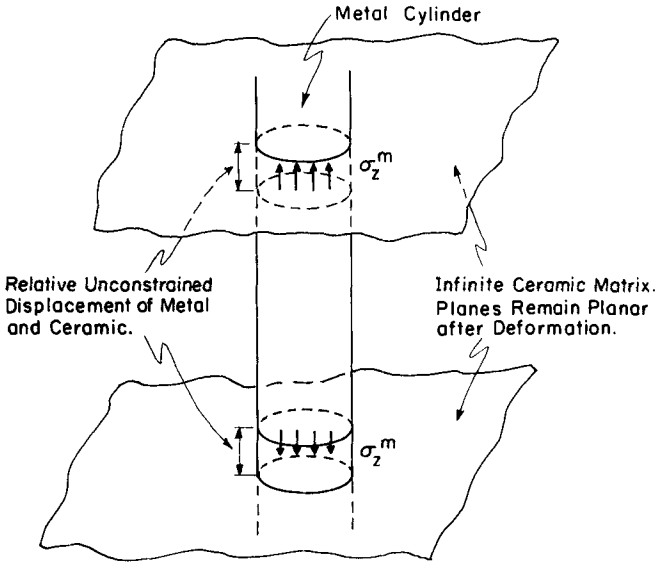

Fig. 4. At a sufficient distance from free surface, a plane parallel to free surface remains parallel during cooling and axial stress in infinite ceramic matrix, σ_z^c, is zero.

of symmetry. The corresponding stresses in the metal are[2]

$$\sigma_r^m = \sigma_\theta^m = \sigma \tag{2}$$

The interface, σ, and the longitudinal, σ_z, stresses are dictated by the boundary conditions and the thermal, elastic/plastic properties of the material. The present analysis is pertinent to the stress away from the surface, wherein planes parallel to the surface remain planar after deformation (Fig. 4). For this condition, a substantial axial stress exists in the metal cylinder.

The total strain within the elastic *matrix* is the sum of thermal and elastic strains, such that

$$\varepsilon_r^c = \alpha_c \Delta T + [(1 + \nu_c)\sigma/E_c](a/r)^2 \tag{3a}$$

$$\varepsilon_\theta^c = \alpha_c \Delta T - [(1 + \nu_c)\sigma/E_c](a/r)^2 \tag{3b}$$

$$\varepsilon_z^c = \alpha_c \Delta T \tag{3c}$$

where α_c is the thermal expansion coefficient, ΔT is the temperature change (ΔT is negative for cooling), and E_c and ν_c are the Young's modulus and Poisson ratio, respectively.

In the *metal*, plastic strains are also involved. These superpose on the thermal and elastic strains given by

$$\varepsilon_r^{mt} = \varepsilon_\theta^{mt} = \varepsilon_z^{mt} = \alpha_m \Delta T \tag{4a}$$

$$\varepsilon_r^{me} = \varepsilon_\theta^{me} = [(1 - \nu_m)\sigma - \nu_m \sigma_z^m]/E_m \tag{4b}$$

$$\varepsilon_z^{me} = [-2\nu_m \sigma + \sigma_z^m]/E_m \tag{4c}$$

The plastic strain is computed by assuming that the plastic deformation in the metal cylinder satisfies the Von Mises criterion[3]

$$\sigma_e \equiv (1/\sqrt{2})[(\sigma_r^m - \sigma_\theta^m)^2 + (\sigma_\theta^m - \sigma_z^m)^2 + (\sigma_z^m - \sigma_r^m)^2]^{1/2} = \sigma_y \tag{5a}$$

where σ_e is the effective stress and σ_y is the yield stress, such that

$$\sigma_e = \sigma_z^m - \sigma \tag{5b}$$

Furthermore, linear work hardening is assumed, whereupon the plastic strain satisfies the Prandtl-Reuss relation[3]

$$d\varepsilon_{ij}^{mp} = \tfrac{3}{2}{}'\sigma_{ij} d\sigma_e/\sigma_e H \tag{6}$$

where H is the slope of the work-hardening curve and ${}'\sigma_{ij}$ are the deviatoric stresses:

$${}'\sigma_{ij} = \sigma_{ij} - \tfrac{1}{3}\sigma_{kk}\delta_{ij} \tag{7}$$

In the present case

$${}'\sigma_r^m = {}'\sigma_\theta^m = \tfrac{1}{3}(\sigma - \sigma_z^m) \tag{8a}$$

$${}'\sigma_z^m = \tfrac{2}{3}(\sigma_z^m - \sigma) \tag{8b}$$

such that

$$d\varepsilon_r^{mp} = d\varepsilon_\theta^{mp} = -\frac{d(\sigma_z^m - \sigma)}{2H} \tag{9a}$$

$$d\varepsilon_z^{mp} = \frac{d(\sigma_z^m - \sigma)}{H} \tag{9b}$$

The stresses can be determined from the strains, subject to the requirements that the displacements be continuous at the interface

$$u_r^m = u_r^c \qquad (r = a) \tag{10a}$$

$$u_z^m = u_z^c \tag{10a'}$$

such that

$$\varepsilon_\theta^m = \varepsilon_\theta^c \qquad (r = a) \tag{10b}$$

$$\varepsilon_z^m = \varepsilon_z^c \tag{10b'}$$

(2) Residual Stresses

The residual stresses can be readily evaluated from the preceding relations, subject to the requirement that the plastic strain ε^p (after

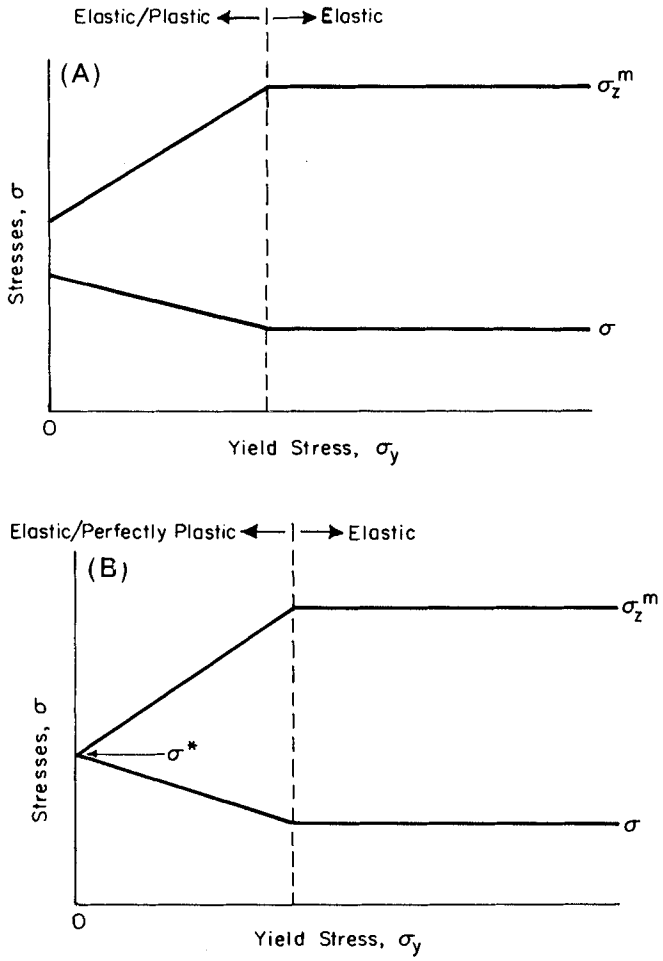

Fig. 5. Interface stress, σ, and axial stress in metal, σ_z^m, as a function of yield stress of metal, σ_y, for (*A*) elastic/plastic material and (*B*) elastic/perfectly plastic material.

yielding initiates) increases monotonically with decrease in temperature, i.e.

$$d|\varepsilon^p|/d(-\Delta T) \geq 0 \tag{11a}$$

or

$$d(\sigma_z^m - \sigma - \sigma_y)/d(-\Delta T) \geq 0 \tag{11b}$$

For this case, the zero plastic strain condition can be referred directly to the yield stress at the current temperature, T. Consequently, integration of Eq. (9) for a material with a temperature independent H gives the plastic strains

$$\varepsilon_r^{mp}(T) = \varepsilon_\theta^{mp}(T) = -[\sigma_z^m(T) - \sigma(T) - \sigma_y(T)]/2H \tag{12a}$$

$$\varepsilon_z^{mp}(T) = [\sigma_z^m(T) - \sigma(T) - \sigma_y(T)]/H \tag{12b}$$

The stresses can now be obtained directly from Eqs. (3), (4), (10), and (12) at temperature T as

$$\sigma(T) = \frac{-(\alpha_m - \alpha_c)\Delta T\left[\frac{(1+\nu_m)}{E_m} + \frac{3}{2H}\right] - \frac{(1-2\nu_m)\sigma_y(T)}{2E_mH}}{\frac{(1-2\nu_m)(1+\nu_m)}{E_m^2} + \frac{3(1-2\nu_m)}{2E_mH} + \frac{(1+\nu_c)}{E_c}\left[\frac{1}{E_m} + \frac{1}{H}\right]} \tag{13a}$$

$$\sigma_z^m(T) = \frac{-(\alpha_m - \alpha_c)\Delta T\left[\frac{(1+\nu_m)}{E_m} + \frac{3}{2H} + \frac{(1+\nu_c)}{E_c}\right] + \frac{\sigma_y(T)}{H}\left[\frac{1-2\nu_m}{E_m} + \frac{1+\nu_c}{E_c}\right]}{\frac{(1-2\nu_m)(1+\nu_m)}{E_m^2} + \frac{3(1-2\nu_m)}{2E_mH} + \frac{1+\nu_c}{E_c}\left[\frac{1}{E_m} + \frac{1}{H}\right]} \tag{13b}$$

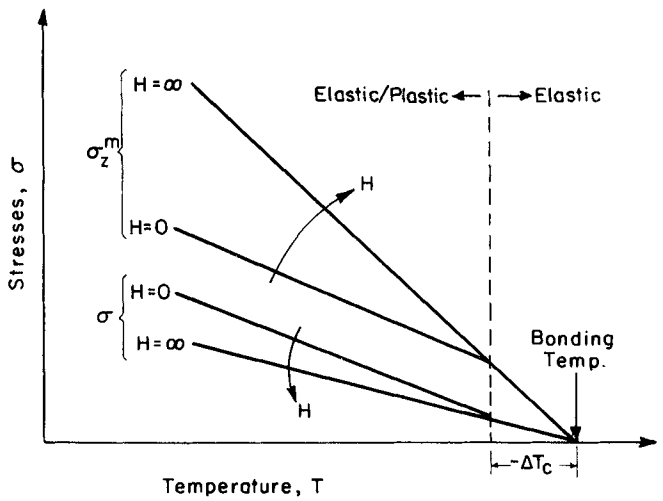

Fig. 6. Interface stress, σ, and axial stress in metal, σ_z^m, as a function of temperature for constant σ_y; also shown are effects of work-hardening rate, H.

where σ_y is the yield strength at the current temperature, T. Terms that relate to the thermal stress $(\alpha_m - \alpha_c)\Delta T$ and to the plastic flow properties (σ_y and H) are evident.

The radial and tangential stresses can be obtained by substituting σ from Eq. (13) into Eqs. (1) and (2). In the absence of work hardening (elastic/perfectly plastic material) the stresses reduce to

$$\sigma = \frac{-3(\alpha_m - \alpha_c)\Delta T - \sigma_y\frac{1-2\nu_m}{E_m}}{\frac{3(1-2\nu_m)}{E_m} + \frac{2(1+\nu_c)}{E_c}} \tag{14a}$$

$$\sigma_z^m = \frac{-3(\alpha_m - \alpha_c)\Delta T + 2\sigma_y\left[\frac{1-2\nu_m}{E_m} + \frac{1+\nu_c}{E_c}\right]}{\frac{3(1-2\nu_m)}{E_m} + \frac{2(1+\nu_c)}{E_c}} \tag{14b}$$

Furthermore, if the temperature change is not large enough to induce plastic deformation of the metal, the stresses are given by the elastic solution

$$\sigma = \frac{-\frac{E_m(\alpha_m - \alpha_c)\Delta T}{1-2\nu_m}\left[\frac{E_c}{1+\nu_c}\right]}{\frac{E_c}{1+\nu_c} + \frac{E_m}{(1+\nu_m)(1-2\nu_m)}} \tag{15a}$$

$$\sigma_z^m = \frac{-\frac{E_m(\alpha_m - \alpha_c)\Delta T}{1-2\nu_m}\left[\frac{E_c}{1+\nu_c} + \frac{E_m}{1+\nu_m}\right]}{\frac{E_c}{1+\nu_c} + \frac{E_m}{(1+\nu_m)(1-2\nu_m)}} \tag{15b}$$

This solution applies subject to the condition

$$-\Delta T \leq \left[1 + \frac{E_c(1+\nu_m)(1-2\nu_m)}{E_m(1+\nu_c)}\right]\frac{\sigma_y}{E_m(\alpha_m - \alpha_c)} \equiv -\Delta T_c \tag{16}$$

The trends in residual stress with yield strength, at fixed ΔT, predicted by Eqs. (13) to (15) are plotted in Fig. 5. In the elastic range, the axial tension exceeds the interfacial stress, by an amount that depends on the relative elastic properties of the metal and ceramic

$$\sigma_z^m/\sigma = 1 + (E_m/E_c)[(1+\nu_c)/(1+\nu_m)] \tag{17}$$

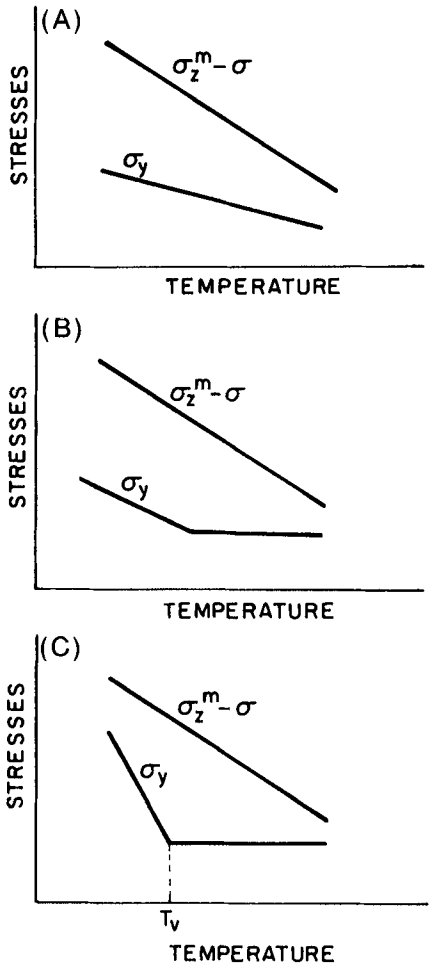

Fig. 7. Schematic illustrating stresses that (*A*),(*B*) satisfy and (*C*) violate requirement that plastic strain increases monotonically with decrease in temperature. In (*C*) the plastic strain remains constant for $T \leq T_v$.

However, when yielding initiates (small σ_y or large $-\Delta T$), the stress difference diminishes due to plastic relaxation of the shape change (Fig. 5). Ultimately, as $\sigma_y \rightarrow 0$, full plastic relaxation of the shape change occurs and for a perfectly plastic material (Fig. 5(*B*)) the axial and interface stresses converge. The convergent stress σ^* is dictated by the dilatational component of the thermal mismatch, such that (for $H = 0$)

$$\sigma^* = -3(\alpha_m - \alpha_c)\Delta T/[3(1 - 2\nu_m)/E_m + 2(1 + \nu_c)/E_c] \quad (18)$$

The corresponding trends in the residual stress for a material with a temperature-independent yield strength are plotted in Fig. 6. Yielding initiates at a critical temperature change, $-\Delta T_c$ (Eq. (16)). However, the stresses continue to increase with further decrease in temperature, due to the increase in dilatational mismatch. Also, note that for materials that exhibit a large work-hardening rate, H, the axial stress is enhanced and the interfacial stress reduced.

(3) Some Effects of a Temperature-Dependent Plastic Flow Stress

The preceding formulation of the residual stresses pertains, as noted above, provided that the metal exhibits continuous plastic straining upon cooling. Some conditions that satisfy and violate this requirement are schematically illustrated in Fig. 7. A specific assessment is conducted for the copper/cordierite ceramic system (Table I) by assuming a linear temperature dependence (Fig. 8), with σ_y varying between 0 at the bonding temperature and

Table I. Physical Properties of Cu and Cordierite Ceramic

Material	Property value			
	E (MPa)	ν	α ($^\circ C^{-1}$)	H (MPa)
Cu alloy	1.3×10^5	0.34	17×10^{-6}	620
Cordierite ceramic	1.3×10^5	0.25	2×10^{-6}	

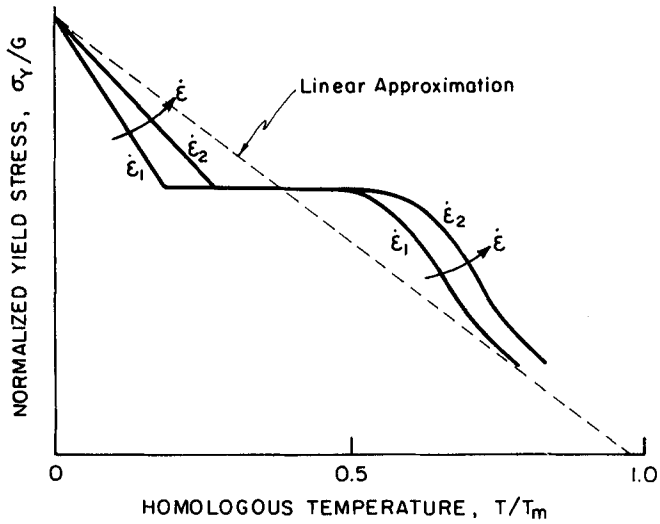

Fig. 8. Schematic showing variation in yield strength with temperature (see Ref. 4) and linear approximation used in present study (G is shear modulus).

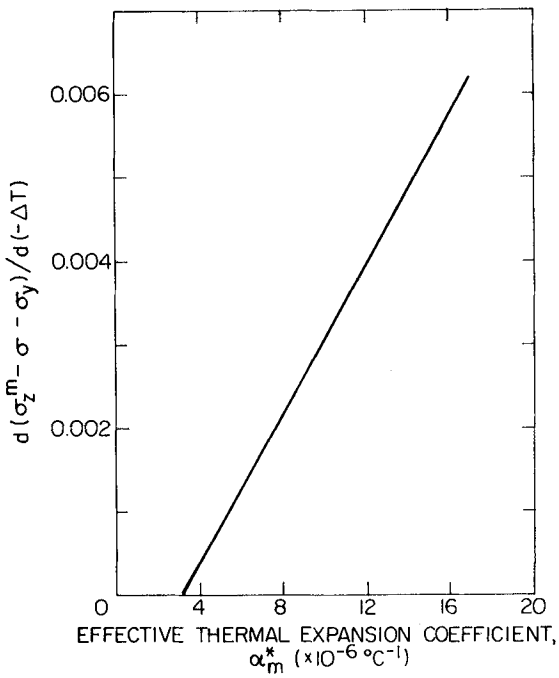

Fig. 9. Requirement $d(\sigma_z^m - \sigma - \sigma_y)/d(-\Delta T) \geq 0$ is satisfied for copper/cordierite ceramic system for $\alpha_m^* > 3.5 \times 10^{-6}$ °C^{-1}.

110 MPa at room temperature. For this case, the stress difference, $\sigma_z^m - \sigma$, deduced from Eq. (13) (with α_m replaced by α_m^*) satisfies the inequality $d(\sigma_z^m - \sigma - \sigma_y)/d(-\Delta T) \geq 0$ (Fig. 9) at all temperatures. Consequently, for this material system, the residual stress formulae based on the current yield strength should be strictly applicable.

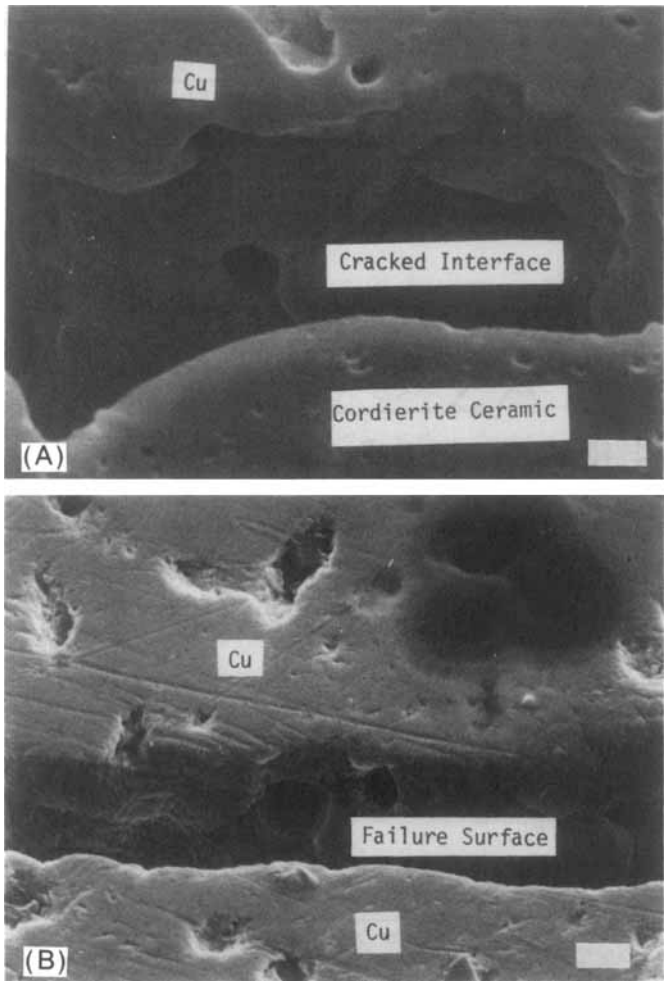

Fig. 10. Scanning electron micrograph (with sample tilt 40°) of pores located on (*A*) cracked interface (bar = 4.15 μm) and (*B*) failure surface of Cu (bar = 5.81 μm).

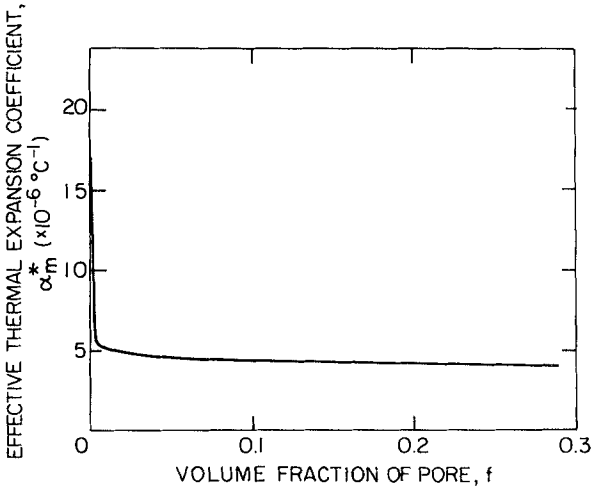

Fig. 11. Effective thermal expansion coefficient of copper, α_m^*, as a function of initial volume fraction of pores, f.

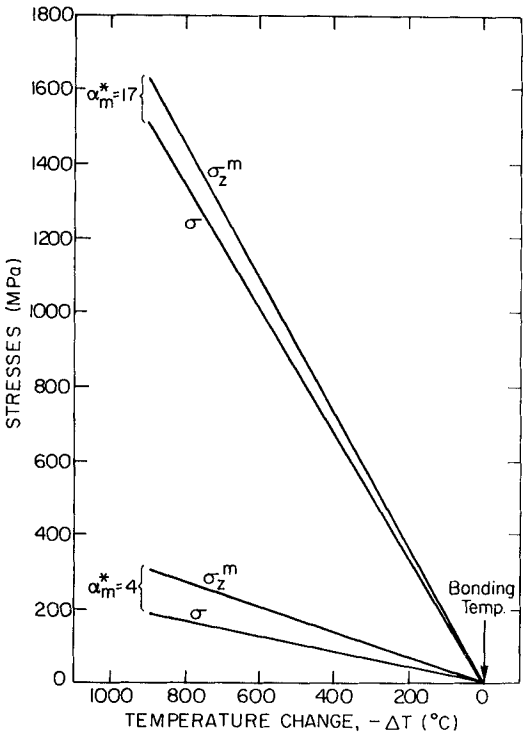

Fig. 12. Stresses that develop in Cu/cordierite ceramic system as a function of temperature change, $-\Delta T$, assuming a linear approximation for yield strength (see Fig. 8), using $\alpha_m^* = 17 \times 10^{-6}$ °C^{-1} and $\alpha_m^* = 4 \times 10^{-6}$ °C^{-1}.

(4) Effects of Porosity

The presence of porosity in the metal (see Fig. 10) may modify the residual stress, by allowing dilatation of the metal, via plastic hole growth.[5-7] This relaxation effect could be substantial for the present, cylindrical geometry, because of the relatively high mean stress.

Approximate account of the role of dilatation may be ascertained by invoking the solution for plastic hole growth in a nonhardening material. Specifically, an isolated spherical pore with volume V subject to an effective remote strain rate, $\dot{\varepsilon}_e$, exhibits a volume expansion rate, $\dot{V}$, given by[6,7]

$$\dot{V}/V = 0.85\dot{\varepsilon}_e \exp(3\sigma_m/2\sigma_y) \tag{19}$$

Assessment of effects of porosity, based on Eq. (19), can be achieved if an expression for the relaxation of the mean stress, σ_m, by the pore expansion be incorporated into the analysis. This is attained, most simply, by replacing the expansion coefficient of the metal with an effective value α_m^*, that remains to be determined by further analysis. This approach assumes, of course, that the pores do not affect the yield criterion, based on the effective stress (Eq. (5)). With this premise, the mean stress can be obtained from Eq. (14) as

$$\sigma_m = \frac{-9(\alpha_m^* - \alpha_c)\Delta T E_c + 2\sigma_y(1 + \nu_c)}{6(1 + \nu_c)} \tag{20}$$

The equivalent effective plastic strain is given by[3]

$$\varepsilon_e^p \equiv \sqrt{2\varepsilon_{ij}\varepsilon_{ij}/3} = -(\alpha_m^* - \alpha_c)\Delta T \tag{21}$$

The plastic strain increment may thus be determined. For the simplified condition of a temperature-independent α_m^* (see Eqs. (24*b*) and (25)).

$$d\varepsilon_e^p = -(\alpha_m^* - \alpha_c)d\Delta T \tag{22}$$

Hence, the pore expansion rates become

$$\int_{V_0}^{V} \frac{dV}{V} = -\int_0^{\Delta T_b} 0.85(\alpha_m^* - \alpha_c) \exp\left[\frac{-9(\alpha_m^* - \alpha_c)\Delta T E_c}{4\sigma_y(1 + \nu_c)} + \frac{1}{2}\right] d(\Delta T) \tag{23}$$

where V_0 is the initial pore volume at the bonding temperature

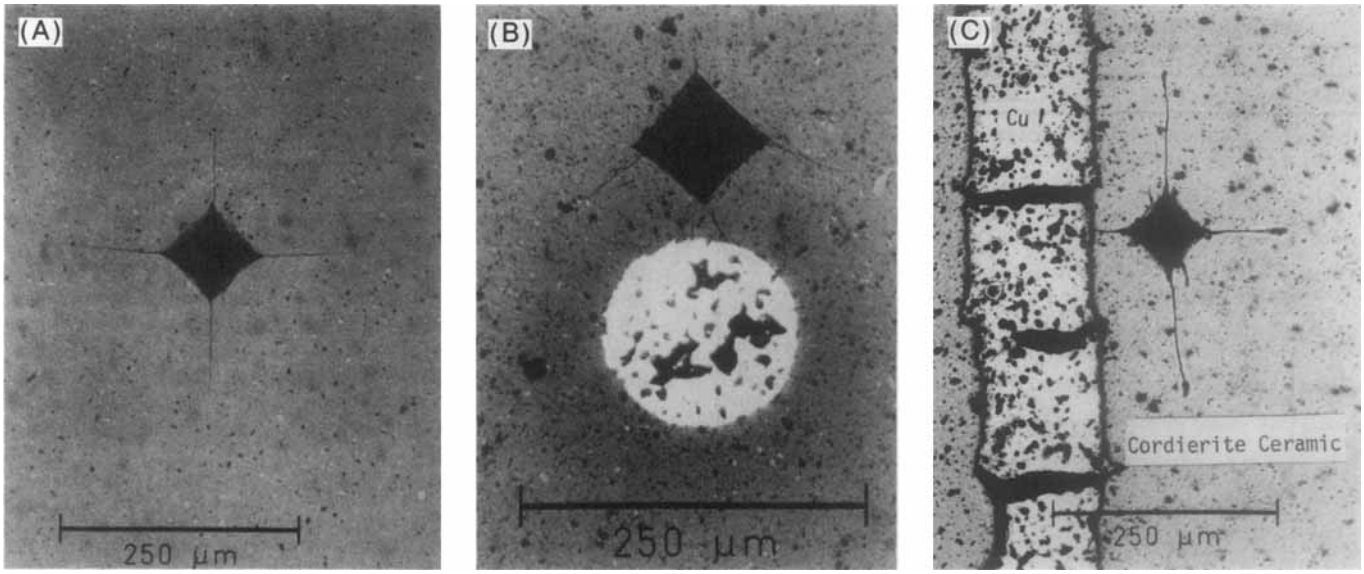

Fig. 13. Indentations emplaced in cordierite ceramic (*A*) remote from copper, showing straight radial cracks, and (*B*),(*C*) adjacent to copper, showing (*B*) normal and (*C*) longitudinal sections of Cu/cordierite ceramic.

($\Delta T = 0$) and ΔT_b is the temperature change from the bonding temperature to room temperature.

Incorporating the temperature-dependent yield characteristics of the metal phase (Fig. 8), the total volume strain in the metal, θ, can be evaluated for noninteracting pores, as

$$\theta \equiv f(V/V_0 - 1) = f\left[\exp\left\{-1.4(\alpha_m^* - \alpha_c)\Delta T_b \times \exp\left[\frac{-9(\alpha_m^* - \alpha_c)E_c \Delta T_b}{4(1 + \nu_c)\sigma_y}\right]\right\} - 1\right] \quad (24a)$$

or

$$\theta \approx -1.4(\alpha_m^* - \alpha_c)\Delta T_b f \exp\left[\frac{-9(\alpha_m^* - \alpha_c)E_c\Delta T_b}{4(1 + \nu_c)\sigma_y}\right] \quad (24b)$$

where f is the volume fraction of initial porosity in the metal. The effective thermal expansion coefficient of the metal then becomes*

$$\alpha_m^* = \alpha_m + \theta/3\Delta T_b \quad (25)$$

The trend in α_m^* with the initial volume fraction of pores, in a Cu/cordierite ceramic system, deduced from Eqs. (24*a*) and (25), is plotted in Fig. 11. Note that, for $f > 0.01$, $\alpha_m^* \approx 4 \times 10^{-6}$ °C^{-1}.

Dilatational effects are thus capable of reducing the stress (Fig. 12) by a substantial factor, ≈8, at relatively small initial porosity levels. Small amounts of porosity in the metal can thus cause appreciable stress relaxation, by acting as nuclei for plastic dilatation.

III. Experimental Studies

(1) Residual Stresses

Residual stresses have been estimated for a copper/cordierite ceramic system, using an indentation technique. With this technique, small Vickers indentations are placed in the ceramic, adjacent to the metal/ceramic interface (Fig. 13). Then, the relative extensions of the radial cracks provide information pertinent to the sign and magnitude of the residual stress. Specifically, in the absence of residual stress, indentation at a load, P, creates a radial crack of radius, c, related to the toughness of the ceramic, K_c, by[8]

$$K_c = \chi P(E/h)^{1/2} c^{-3/2} \quad (26)$$

where E and h are the modulus and hardness of the ceramic and χ is a coefficient equal to 0.016. In the presence of residual stress, the crack length and geometry are modified, such that the residual stress, σ_R, and the crack radius, c_*, are related to the toughness by

$$K_c = \chi_* P(E/h)^{1/2} c_*^{-3/2} + \sigma_R \Omega c_*^{1/2} \quad (27)$$

where Ω is a coefficient that depends on the uniformity of the residual field (for a uniform field, $\Omega = 2/\sqrt{\pi}$). The residual stress, σ_R, can be related to the metal/ceramic interface stress, σ, by

$$\sigma_R = \sigma(r/a)^{-2} \quad (28)$$

Hence, by first evaluating K_c from indentations placed at locations remote from the metal (Fig. 13(*A*)), the interface residual stress, σ, may be estimated from radial crack lengths measured at indentations placed at various radial positions, adjacent to the interface.

Inspection of cracking patterns around normal and longitudinal sections reveals (Figs. 13(*B*) and (*C*)) that the circumferential or axial cracks are relatively enlarged, while the radially oriented cracks are suppressed. A condition of radial tension and circumferential compression is thus implied, consistent with the larger thermal expansion of the copper.

Determination of the toughness of the cordierite ceramic from remote indentations indicates that $K_c = 1.4$ MPa·m$^{1/2}$. With this toughness, the interfacial residual tension can be determined from the radial crack lengths (as measured on the normal section) as $\sigma = 130$ MPa ($\chi_* = 0.009$).

(2) Flow Stress of Metal

The flow stress of the metal cylinder can also be estimated with indentation techniques. In this instance, impressions are made with pyramidal indentors having various profiles, with included angle ϕ. Then the flow stress, σ_f, is related to the load, P, and the indentation cross section, A, by[9]

$$\sigma_f \approx P/3A \quad (29)$$

while the corresponding plastic strains, ε_p, for each included angle, ϕ, are given in Table II.[10] Data obtained by using in-

*Note that, with the linear approximation for the temperature dependence of the yield strength (Fig. 8), $\sigma_y/\Delta T_b$ is constant and α_m^* is thus independent of temperature, consistent with our initial premise.

Table II. Plastic Strains Generated by Indentation

Indenter angle, ϕ (degrees)	60	90	120	140	160
Plastic strain, ε_p	0.3	0.25	0.17	0.1	0.06

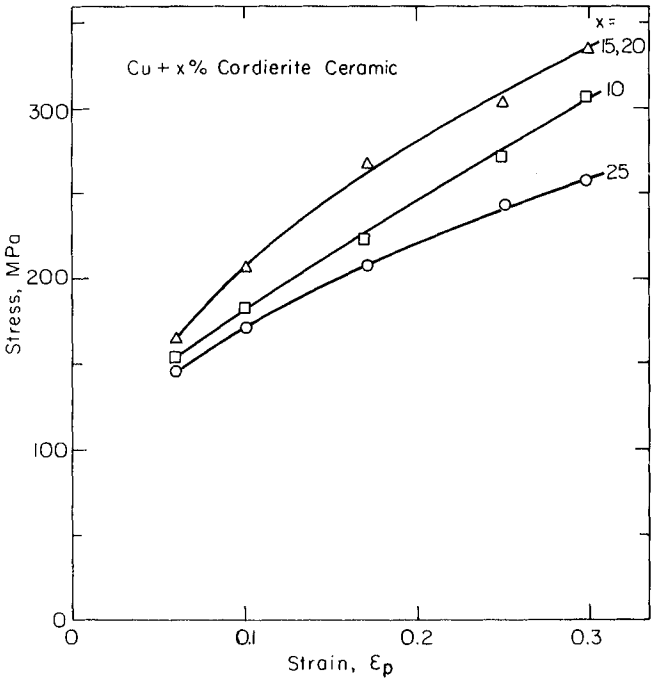

Fig. 14. Stress-strain curves of copper alloys obtained from indentation tests.

cluded angles between 60° and 160° result in the flow stress trends summarized in Fig. 14.

(3) Mechanical Damage

Two primary modes of damage have been observed in the copper/cordierite ceramic system. Interface decohesion (Fig. 15(*B*)) has been identified at a small fraction of normal and longitudinal sections. Ductile fracture of the copper has also been detected (Fig. 15(*C*)) at various axial locations. These modes of damage are induced by the tensile residual stresses in the radial and axial directions, respectively. Appreciable porosity is also observed throughout the copper phase (Fig. 10).

(4) Remarks on Residual Stresses

The plastic flow properties of the copper measured at room temperature can be used in conjunction with the elastic properties

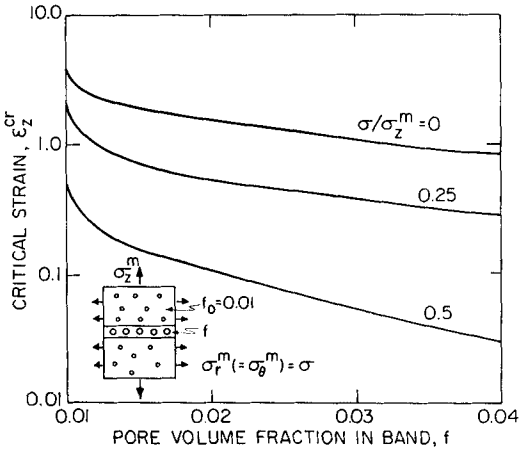

Fig. 16. Critical strain, ε_z^{cr}, for onset of plastic flow localization in infinite band perpendicular to direction of maximum principal stress, σ_z^∞, vs pore volume fraction in band, f, for stress triaxialities indicated (see Ref. 11).

of the copper and cordierite ceramic to compute the residual stresses, from the analysis presented in Section II. An interface residual stress, σ = 1500 MPa, is obtained. This stress is substantially in excess of the measured stress (σ = 130 MPa), because the residual stresses have been measured on the surface, where $\sigma_z = 0$ applies. On the surface the stresses are determined exclusively by the plastic flow stress, as confirmed by the similarity in the present measurements of the residual stress and the plastic flow stress (Fig. 14). However, the residual stress may also be appreciably less than the calculated stress of 1500 MPa, due to plastic dilatation of the pores in the copper (Fig. 15). As estimated in Section II(4), porosity in excess of ≈0.01 can reduce the residual stress by a factor of ≈8; a reduction which coincidentally results in a stress similar to the measured stress. It is thus concluded that porosity in the copper should allow appreciable relaxation of the residual stress.

The residual stress can be further minimized by undercooling and then reheating the system.[12] The final stresses are the sum of Eq. (13) (with ΔT as the undercooling temperature) and Eq. (15) (with ΔT_h, the positive reheat temperature).

Initial porosity in the copper may also have the detrimental effect of inducing premature ductile rupture (Fig. 15(*C*)). Void clusters are capable of initiating ductile rupture by means of a plastic instability.[11] The rupture strain depends on the initial fraction of voids and the triaxiality (Fig. 16). Consequently, since the triaxiality is relatively large in this case, $\sigma/\sigma_z \approx 0.67$, premature ductile rupture would be encouraged by local void clusters in the copper. A homogeneous distribution of initial porosity in the copper is evidently needed to inhibit local ductile rupture, while still permitting stress relaxation.

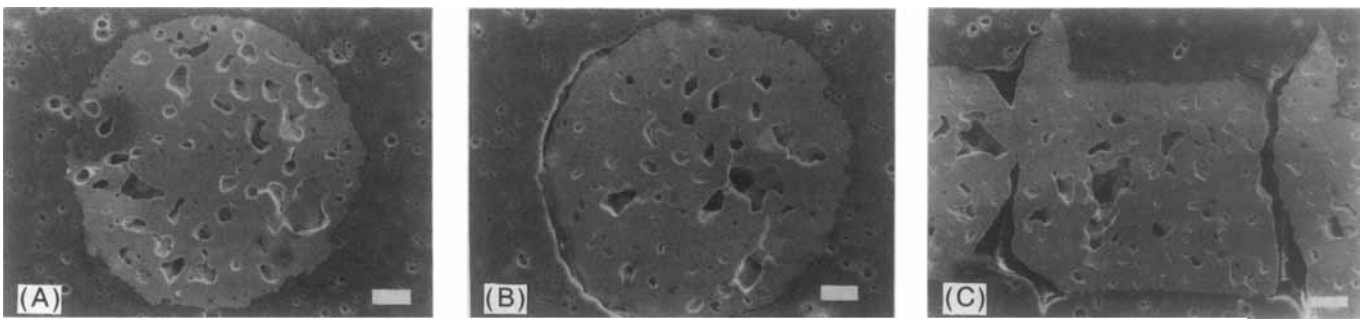

Fig. 15. (*A*) Perfect bonding of metal/ceramic (bar = 17.8 μm) and (*B*),(*C*) failure modes in metal/ceramic showing (*B*) interface decohesion (bar = 17.7 μm) and (*C*) ductile failure of metal (bar = 23.8 μm).

IV. Conclusions

A stress analysis was conducted for a linear work-hardening metal cylinder embedded in an infinite ceramic matrix. The bond between the metal and ceramic is established at high temperature and stresses develop during cooling to room temperature. The calculations show that the stresses depend on the mismatch in thermal expansion, the elastic properties, and the yield strength and work-hardening rate of the metal. Experimental measurements of the surface stresses have also been made on a Cu/cordierite ceramic system, using an indentation technique. A comparison reveals that the calculated stresses are appreciably larger than the measured surface stresses, indicating an important difference between the bulk and surface residual stresses. However, it is also shown that porosity in the metal can plastically expand and permit substantial dilatational relaxation of the residual stresses. Conversely it is noted that pore clusters are capable of initiating ductile rupture, by means of a plastic instability, in the presence of appreciable triaxiality. A homogeneous distribution of porosity in the metal is thus needed.

References

[1]A. J. Blodgett, Jr., "Microelectronic Packaging," *Sci. Am.*, **249** [1] 86–96 (1983).
[2]S. Timoshenko and J. N. Goodier, Theory of Elasticity. McGraw-Hill, New York, 1951.
[3]R. Hill, "The Mathematical Theory of Plasticity," Clarendon Press, Oxford, 1950.
[4]A. G. Evans and T. G. Langdon, "Structural Ceramics," *Prog. Mater. Sci.*, **21** [3–4] 171–441 (1976).
[5]F. A. McClintock, "A Criterion for Ductile Fracture by the Growth of Holes," *J. Appl. Mech.*, **35** [2] 363–71 (1968).
[6]J. R. Rice and D. M. Tracey, "On the Ductile Enlargement of Voids in Triaxial Stress Fields," *J. Mech. Phys. Solids*, **17** [3] 201–17 (1969).
[7]B. Budiansky, J. W. Hutchinson, and S. Slutsky; pp. 13–45 in Mechanics of Solids, The Rodney Hill 60th Anniversary Volume. Edited by H. G. Hopkins and M. J. Sewell. Pergamon Press, Oxford and New York, 1982.
[8]D. B. Marshall and B. R. Lawn, "Flaw Characteristics in Dynamic Fatigue: The Influence of Residual Contact Stresses," *J. Am. Ceram. Soc.*, **63** [9–10] 532–36 (1980).
[9]F. P. Bowden and D. Tabor, The Friction and Lubrication of Solids. Clarendon Press, Oxford, 1964.
[10]A. G. Atkins and D. Tabor, "Plastic Indentation in Metals with Cones," *J. Mech. Phys. Solids*, **13** [3] 149–64 (1965).
[11]N. Ohno and J. W. Hutchinson, "Plastic Flow Localization due to Non-Uniform Void Distribution," *J. Mech. Phys. Solids*, **32** [1] 63–85 (1984).
[12]C. H. Hsueh and A. G. Evans, "Residual Stresses in Metal/Ceramic Bonded Strips"; to be published in *J. Am. Ceram. Soc.*

J. Am. Ceram. Soc., **68** [3] 127–130 (1985)

Stresses in Dumet-Glass Seals

A. K. VARSHNEYA* and J. E. MARRA*

New York State College of Ceramics at Alfred University, Alfred, New York 14802

Hull and Burger's calculations of stresses in the Dumet-glass bead seals, which were based on Poritsky's erroneous analysis, are corrected. Copper yielding is properly introduced. Calculated anisotropic thermal expansion of two types of Dumet alloy, as well as stresses in Dumet wire-soft lead glass bead seals are in good agreement with those measured experimentally. Metal composites suitable for glass sealing can be formulated by using the analysis presented.

I. Introduction

THERMAL contraction coefficients of most so-called "soft glasses" are generally around 90 to 100 × 10^{-7}/°C. Typical soft glasses used in glass-to-metal seals are, for instance, GE 001 and GE 012 (both "potash soda lead" glasses) and GE 008 (a "soda lime" glass). It happens that Pt is the only pure metal which has a reasonable expansion match (differential contractions <500 ppm) with either of the three soft glasses (see, for instance, comparison of the expansion of GE 001 with several metals in Fig. 1). The cost of Pt, however, renders Pt-soft glass seals quite prohibitive to large-scale manufacture. Although alloys such as 52% Ni-Fe and Sylvania 4 are a good match to soft glasses and are inexpensive, their usage in electrical applications has been limited because of poor soderability to refractory metals such as W and Mo.

In 1913, B. E. Eldred invented the Dumet alloy for sealing to soft glasses (U.S. Pat. Nos. 1 140 134–136). It consisted of a core of approximately 38 to 42% Ni-Fe alloy and a thin copper cladding. The Cu cladding allowed direct soldering to W and Mo. The proportion of Cu was about 18 to 25 wt% and could be adjusted such that the "average expansion" of the composite wire matched that of a given batch of glass. Eldred also pointed out that the addition of Cu also "regularized" (or straightened out the knee) in the expansion of Ni-Fe alloy wires (see Fig. 1), thus reducing the risk of glass fracture during cooling.

Both copper and Ni-Fe alloy have isotropic thermal expansions; however, Dumet does not. Eldred paid little attention to this anisotropy and merely desired to have the average expansion of the composite be somewhat lower than, but still a close match to, that of the glass.

In 1934, Hull and Burger[1] first attempted a calculation of the effective thermal expansion of the Dumet alloy and stresses in Dumet-soft glass seals. They used Poritsky's[2] bead seal stress formulae to arrive at the following conclusions:

Presented at the 84th Annual Meeting and Exposition, The American Ceramic Society, Chicago, IL, April 26, 1983 (Glass Division, Paper No. 49-G-83). Received September 6, 1983; revised copy received May 21, 1984; approved September 21, 1984.

Based in part on the thesis submitted by J. E. Marra for the degree of B.S. in Ceramics at Alfred University.

*Member, the American Ceramic Society.